

# Iterative run-time bias corrections in an atmospheric GCM (LMDZ v6.3)

Gerhard Krinner<sup>1</sup>, Aude Champouillon<sup>1,2</sup>, Juliette Blanchet<sup>1</sup>, and Frédérique Chéruy<sup>3</sup>

<sup>1</sup>Univ. Grenoble Alpes, CNRS, INRAE, IRD, IGE, 38000 Grenoble, France

<sup>2</sup>École nationale des ponts et chaussées, Institut Polytechnique de Paris, 77455 Marne-la-vallée, France

<sup>3</sup>Laboratoire de Météorologie Dynamique-IPSL, Sorbonne Université/CNRS/École Normale Supérieure-PSL Université/École Polytechnique-Institut Polytechnique de Paris, Paris, France

**Correspondence:** Gerhard Krinner (gerhard.krinner@cnr.fr)

**Abstract.** Run-time bias corrections of atmospheric circulation models can be based on nudging (Newtonian relaxation) to an atmospheric reanalysis. In this case, the time increments of selected state variables are modified by adding the nudging terms obtained with an uncorrected version of the model. This is a well-known method to improve the models' representation of large-scale circulation patterns. In this work, we propose and evaluate a variant of this method, consisting of iterative nudging: the corrected model is itself nudged towards the reanalysis, and the resulting nudging terms are added to the initial ones to calculate the new, iterated correction terms. This procedure can be iterated an arbitrary number of times. Evaluating the LMDZ atmospheric general circulation model (AGCM) for a varying number of iterations of nudging to the ERA5 reanalysis for the period 1981-2000, we show that the simulated large-scale circulation patterns over the period 2001-2020 are consistently improved when the bias correction procedure is iterated compared to the non-iterated original procedure. However, signs of over-correction appear after about three iterations.

## 1 Introduction

Despite constant and continuing progress over several decades, climate models (in a broad sense, ranging from Earth System Models to limited-area dynamical atmospheric circulation models) still exhibit biases in their representation of current climate and of large-scale indicators of climate change (Eyring et al., 2021; Arias et al., 2021). Nevertheless, in the face of rapid climate change and its increasingly detrimental impacts, climate models remain the primary source of information to quantify future climate change from global to regional scales (Lee et al., 2023). However, for most use cases, run-time bias corrections of climate models, or bias adjustments of their output, are necessary (Doblas-Reyes et al., 2021; Ranasinghe et al., 2021).

The type of empirical run-time bias corrections (ERBC) that is used in the present work has, to our knowledge, first been described for atmospheric general circulation models by Guldberg et al. (2005), building on earlier work with simplified models (D'Andrea and Vautard, 2000) that already contains the main ideas. In this approach, time increments to the model's state variables are corrected using terms derived from the corrected increments that are obtained using a simulation that is nudged to atmospheric analyses or, more frequently, reanalyses (see Section 2). A number of studies have used this approach,

or slight variations thereof (e.g., Bloom et al., 1996), to reduce systematic model errors in a weather or seasonal prediction context (e.g., Kharin and Scinocca, 2012; Chang et al., 2019).

25 Nudging as such, without the additional ERBC step building on it, is a frequently used technique for climate model evaluation (e.g., Sun et al., 2019; Zhang et al., 2022; Pithan et al., 2023). Notably, despite the frequent use of nudging in climate models, the specific implementation strategy and parameter choices (in particular, the nudging strength) need to be carefully chosen and evaluated (e.g., Zhang et al., 2014).

Here we use the nudging-based ERBC approach to reduce climate model biases with the explicit intention to produce bias-  
30 corrected climate projections as, for example, in Krinner et al. (2019). In a perfect model framework, the nudging-based ERBC approach has been shown to substantially improve simulated future climate projections (Krinner et al., 2020). Together with the fact that even in the context of a strong climate change ( $4\times\text{CO}_2$ ), large-scale climate model bias patterns have been shown to be stationary to a high degree (Krinner and Flanner, 2018), this justifies the use of this method, for example, for projections of future Antarctic climate on a centennial time scale (Krinner et al., 2019; Beaumet et al., 2019). Compared to post-hoc  
35 bias adjustment of climate model output, a potential advantage of run-time bias corrections is that the improved large-scale circulation patterns can lead to a more physically consistent multivariate representation of climate change. Moreover, even if the output of a climate model using such a run-time bias correction method may require further statistical bias correction because necessarily some biases remain (e.g., Scinocca and Kharin, 2024), a better representation of large-scale circulation patterns may help avoid pitfalls of post-hoc statistical bias corrections linked to the misplacement of critical circulation features  
40 (e.g., Hall, 2014; Maraun et al., 2017).

Nudging-based run-time bias corrections only partly eliminate model biases. Root mean square error (RMSE) reductions of about 30-50% are typical for this method (Krinner et al., 2020; Scinocca and Kharin, 2024), depending on the model and the assessed variable. This is the main reason why in this paper, we examine the question whether an iterative application of this method can lead to a more effective bias reduction. However, as with any model tuning or bias correction, care has to be  
45 taken to avoid over-correction of model biases. The aims of this paper are therefore a) to describe the iterative bias correction procedure implemented in the LMDZ6 atmospheric GCM (Hourdin et al., 2020); b) to evaluate the simulated present-day climate in the uncorrected model and for a varying number of iterations of the correction procedure; c) to determine limits of the procedure, in particular by identifying possible signs of over-correction.

The next section describes the iterative run-time bias correction method and the simulations carried out to test it. We then  
50 present results for circulation-related variables on large spatial and varying temporal scales, and discuss the potential of the method and its limitations, as well as limitations of the present work.

## 2 Methods

### 2.1 Iterative run-time bias correction

We start from the “classical” nudging-based run-time bias correction method described by Guldberg et al. (2005). Following  
55 the notation used by Scinocca and Kharin (2024), the original model increments for a state variable  $X$  (e.g. the meridional or

zonal wind component) are noted  $M(X, t)$ :

$$\partial_t X = M(X, t). \quad (1)$$

When the model is nudged (Jeuken et al., 1996) to a (re)analysis, these time-varying model increments become:

$$\partial_t X = M(X, t) + \frac{X_a - X}{\tau} \equiv N_0(X, t), \quad (2)$$

60 where  $X_a$  denotes the reanalysis state variable,  $\tau$  the nudging timescale (here, 1 day), and  $N_0$  the nudged version of the model. The influence and the choice of the nudging time constant is discussed in section 4.2. The nudging strength is reduced to 0 near the surface (using a hyperbolic tangent factor transitioning from close to 1 to close to 0 over a range of about 500 m around 1500 m above the surface, and similarly at the upper limit of the atmosphere (beyond 5 hPa)).

The climatological nudging increments  $G_0 = \overline{(X_a - X)}/\tau$  (the overbar denoting a cyclostationary time average, taking into  
65 account seasonal and daily cycles) are then used in a bias-corrected simulation denoted  $C_0$ :

$$\partial_t X = M(X, t) + G_0 \equiv C_0(X, t), \quad (3)$$

where  $G_0$  is a function of space (latitude, longitude and vertical level) and time (day of the year). To reduce the high-frequency weather noise generated by averaging over only 20 years for any given day of the year, we apply a 20-day running-mean average to the final correction terms, but preserve the mean daily cycle.

70 Until this stage, this is, as stated, the “classical” run-time bias correction method described by Guldberg et al. (2005).

We can now simply iterate this procedure for a first time, using the initial corrected model  $C_0$ :

$$\partial_t X = C_0(X, t) + \frac{X_a - X}{\tau} \equiv N_1(X, t). \quad (4)$$

Here,  $N_1$  stands for the first iterated nudging. The cyclostationary climatological nudging increments  $G_1 = \overline{(X_a - X)}/\tau$  of this first iteration are then added to the initial correction terms  $G_0$ :  $G_{0+1} = G_0 + G_1$ . The first iterated corrected model run  $C_1$   
75 then uses these combined correction terms:

$$\partial_t X = M(X, t) + G_{0+1} \equiv C_1(X, t). \quad (5)$$

This iteratively corrected model can then again be nudged to the (re)analysis. In general terms, the  $n^{\text{th}}$  iteration of the bias-corrected model is then given by:

$$\partial_t X = M(X, t) + G_{0+1+\dots+n} \equiv C_n(X, t). \quad (6)$$

80 Because the nudging timescale  $\tau$  is of the order of days (here, 1 day) and the model timestep of the order of minutes, the initial correction term  $G_0$  derived from equation 2 only partially offsets the model’s systematic drift relative to the reanalysis. Similarly, the subsequent correction terms  $G_{0+1}$  and more generally  $G_{0+1+\dots+n}$  only partially offset this systematic drift. The question of potential convergence is addressed in subsection 3.1.

## 2.2 Simulations and analysis

85 We use the LMDZ6 AGCM (Hourdin et al., 2020) at low resolution ( $96$  (longitude)  $\times$   $95$  (latitude) horizontal grid points and  
79 vertical levels), coupled to the ORCHIDEE land surface model (Krinner et al., 2005). The model is nudged towards the  
ERA5 reanalysis (Hersbach et al., 2020) for the period 1981-2000 (plus the year 1980 for model spinup). Only the meridional  
and zonal wind components above about  $P = 0.85P_s$  (where  $P$  and  $P_s$  are the atmospheric pressure at a given level and at the  
surface, respectively) are nudged towards ERA5 with a time constant of  $\tau = 1$  day in the nudged simulations  $N_i$  ( $i = 0 \dots 3$ ).  
90 The corrected simulations  $C_i$  ( $i = 0 \dots 3$ ) and the uncorrected control simulations, denoted M, are run for the evaluation period  
2001-2020 (plus the year 2000 for model spinup), distinct from the nudging period. These simulations are run twice, starting in  
2000 with varying initial conditions. For these simulations we use atmospheric states obtained from other uncorrected LMDZ  
simulations for the years 1995 and 2000, respectively, and discard the first year of the integration as spinup, as just mentioned.  
The presented results for these simulations M and  $C_i$  are the average of these  $2 \times 20 = 40$  model years. Table 1 provides a  
95 summary of the simulations described in this work.

Simulation	Type	Period
M	Uncorrected, free-running	2001-2020 (2 runs)
$N_0$	Uncorrected, nudged to ERA5	1981-2000
$C_0$	Corrected using $N_0$ , free-running	2001-2020 (2 runs)
$N_1$	Corrected using $N_0$ , nudged to ERA5	1981-2000
$C_1$	Corrected using $N_0+N_1$ , free-running	2001-2020 (2 runs)
$N_2$	Corrected using $N_0+N_1$ , nudged to ERA5	1981-2000
$C_2$	Corrected using $N_0+N_1+N_2$ , free-running	2001-2020 (2 runs)
$N_3$	Corrected using $N_0+N_1+N_2$ , nudged to ERA5	1981-2000
$C_3$	Corrected using $N_0+N_1+N_2+N_3$ , free-running	2001-2020 (2 runs)

**Table 1.** Simulations discussed in detail in this work.

In the Discussion, we briefly refer to one additional iteratively bias-corrected, supplementary test simulation that uses a nudging timescale of  $\tau = 3$  d.

100 Evaluation is carried out against 2001-2020 ERA5 circulation characteristics such as climatological mean biases for meridional ( $v$ ) and zonal ( $u$ ) wind at selected standard pressure levels (850, 500 and 200 hPa), mean sea-level pressure biases, inter-annual patterns of sea-level pressure variability using empirical orthogonal functions, blocking frequencies (Davini et al., 2012; Palmer et al., 2023) based on 500 hPa geopotential indices, band-pass (between 2.5 and 7d) sea-level pressure variability linked to storm track location and intensity (Chang, 2009), and frequencies of synoptic weather patterns using 5x4 self-organizing maps (Kohonen, 1982) of hemispheric extratropical (polewards of  $40^\circ\text{N}$  and S) daily-mean geopotential heights. Furthermore, the amplitude of the  $u$  and  $v$  correction terms is analyzed to evaluate convergence of the correction procedure.

105 Contrary to previous studies (Krinner et al., 2019, 2020), we refrained from bias-correcting atmospheric temperatures be-  
cause we have realized that run-time temperature bias corrections in the LMDZ AGCM destructively interfere with the physical  
parameterizations in the tropics. In particular, the temperature corrections significantly reduce a large-scale tropospheric cold  
bias in the model, leading to reduced convective instability and thus to reduced simulated convective activity, accumulation  
of water vapour in the atmospheric boundary layer, and a substantial surface energy flux imbalance linked to reduced surface  
110 evaporation and increased downwelling longwave radiation.

### 3 Results

#### 3.1 Nudging and correction increments

The amplitude of the nudging increment decreases for higher iterations, as shown in Figure 1 for the zonal mean absolute zonal  
wind nudging increments. While the spatial patterns are broadly similar for all simulations  $N_i$ , the amplitude of the nudging  
115 increments decreases by approximately a factor of 2–3 from  $N_0$  to  $N_3$ . Contrary to the nudging increments, which decrease,  
the amplitude of the bias correction increments applied in simulations  $C_i$  increases for higher iterations, as the correction  
increments  $G_{0+\dots+i}$  for simulation  $C_i$  are the sum of the average nudging increments of  $N_0$  to  $N_i$  (see Equation 6). The spatial  
structure of the bias correction increments  $G_{0+\dots+i}$  also remains similar for the successive iterations  $C_i$ , but for the higher  
iterations it is not a simple spatially constant multiple of the initial correction increments  $G_0$  used for  $C_0$ , as shown by the ratio  
120 of the zonal mean absolute zonal wind correction increments between  $G_{0+\dots+3}$  and  $G_0$ , displayed in Figure 2. Instead, this  
ratio has distinctive spatial structures varying in space and in time through the annual cycle (not shown), indicating that the  
iterative procedure is not identical to a simple uniform amplification of the initial correction. We interpret this as being linked  
to the non-linear and non-local nature of the atmospheric system, where the bias corrections implemented during a correction  
step can increase tendency errors elsewhere, which are then corrected during the next iteration, and where spatially unequal  
125 bias reduction at one iteration can also lead to modified tendency errors, and thus subsequent bias reduction, in the following  
iteration.

Do these successive correction terms converge towards some “final” correction term? Figure 1d shows that the nudging  
increments in the third iterated nudging step  $N_3$  do not vanish, although they are substantially weaker than in  $N_0$  (Figure 1a).  
The global mean of the absolute zonal wind nudging tendencies (in January, to be consistent with Figure 1) is 0.50 m/s/day for  
130  $N_0$ , 0.35 m/s/day for  $N_1$ , 0.29 m/s/day for  $N_2$ , and 0.26 m/s/day for  $N_3$ . This means that the intensity of the remaining nudging  
tendencies decreases at higher iterations, but convergence towards potentially vanishing final nudging tendencies is still far  
away after 3 iterations. The combined correction terms arising from the sum of these absolute zonal wind nudging tendencies  
have global mean values of 0.50 m/s/day for  $G_0$  (because  $G_0$  is identical to the mean nudging tendencies of  $N_0$ ), 0.83 m/s/day  
for  $G_{0+1}$ , 1.09 m/s/day for  $G_{0+1+2}$ , and 1.30 m/s/day for  $G_{0+\dots+3}$ , and are thus somewhat lower than the corresponding  
135 sums of the global mean of the absolute zonal wind nudging tendencies (which would be 0.5, 0.85, 1.14 and 1.40 m/s/day,  
respectively), indicating that some local-scale compensation occurs between different iterations, as already shown by Figure 2.

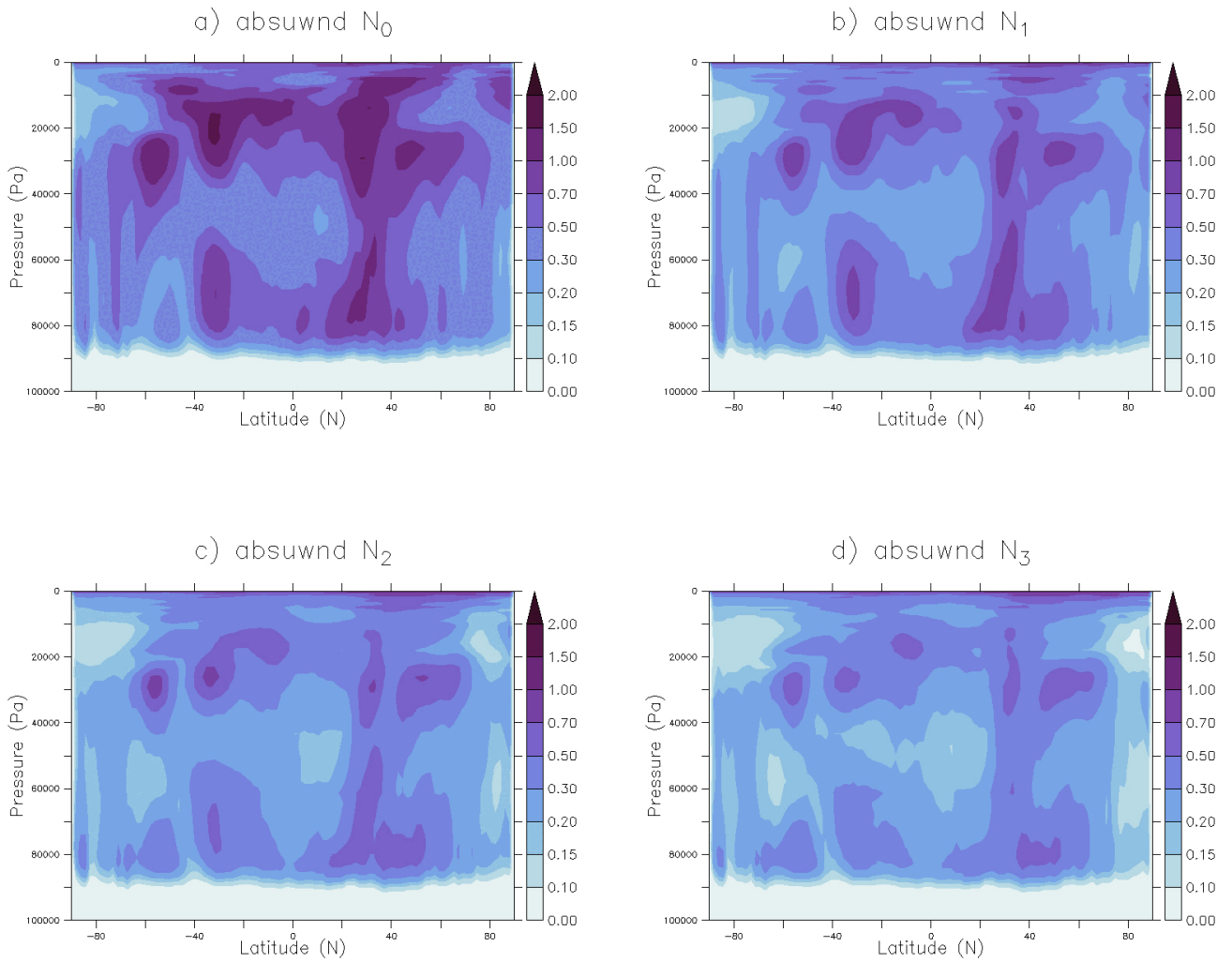


**Figure 1.** Zonal mean absolute zonal wind nudging increments (in m/s/day) calculated from a)  $N_0$  (used in  $C_0$ ); b)  $N_1$ ; c)  $N_2$ ; d)  $N_3$ , average for January 1981 to 2000.

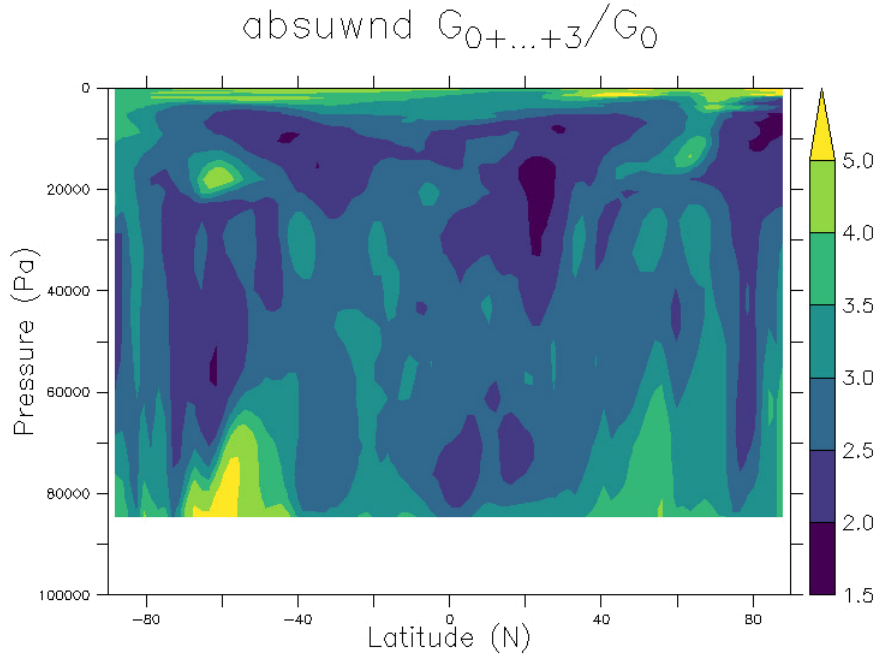


**Figure 2.** Ratio of the zonal mean absolute zonal wind bias correction terms (averages for January 1981 to 2000) between those used in  $C_3$  (bias correction terms  $G_{0+\dots+3}$ ) and those used in  $C_0$  (bias correction terms  $G_0$ ). Values between 100000 and 85000 Pa are not shown in the lower part of the figure. They are not relevant as, by construction, the absolute values of the increments vanish at these altitudes (see Figure 1).

### 3.2 Mean errors

Plots for wind bias reductions obtained with the standard bias correction method and its successive iterations are provided in Figure 3 (maps for  $u$  at 500 hPa) and in Figure 4 (zonal means for  $u$  and  $v$ ). Figure 3 displays the 1981–2000 annual mean bias of the zonal wind component at 500 hPa for the different simulations. Figure 4 displays, in each of its two panels, the ratio of the 1981–2000 RMSE in each of the corrected simulations  $C_i$  ( $i = 0, \dots, 3$ ) and the RMSE of the uncorrected control simulation M:  $\text{RMSE}(C_i)/\text{RMSE}(M)$ , for the annual mean of the zonal (a) and meridional (b) wind speed, where the RMSE is calculated with respect to ERA5.

By construction, mean wind biases at various levels in the atmosphere are decreased in the corrected simulation  $C_0$  compared to the uncorrected control simulation M. Relative to M, the RMSE of the zonal and meridional wind components  $u$  and  $v$  is decreased by  $\approx 20\%$  near the atmospheric boundary layer (where no correction is applied) to  $\approx 60\%$  (for  $u$ ) at 200 hPa. When

the correction procedure is iterated once (simulation  $C_1$ ), a further substantial RMSE reduction is obtained. In most cases except close to the atmospheric boundary layer, no substantial further improvement is obtained in subsequent iterations of the correction procedure.

150 In the absence of run-time temperature corrections in this study, substantial large-scale air temperature biases remain in our wind-only corrected simulations  $C_i$  (see Figure 5). While the wind corrections lead to improvements in the zonal-mean temperature simulation in the upper atmosphere, above  $\approx 300$  hPa, the bias reduction is only modest below this level. In addition, further bias reduction between 200 and 300 hPa in polar regions during higher iterations ( $>2$ ) of the bias correction procedure come at the expense of a degradation of the simulated temperature patterns at these latitudes at about 150 hPa. Because the  
155 wind corrections act through the model dynamics, its influence on temperature is expected to arise primarily through dynamical balance (e.g. thermal wind, geostrophic and hydrostatic adjustment), which constrains horizontal temperature gradients rather than the global-mean temperature at a given pressure level. As a result, wind-only bias correction can reasonably be expected to improve regional temperature anomalies about the level-wise global mean while leaving the global-mean temperature largely unaffected, since the latter is controlled by the column-integrated energy balance and model physics. Therefore, when for a  
160 given pressure level the global mean bias is accounted for (i.e. subtracted, yielding a centered temperature  $\tilde{T} = T - \Delta T$ , where  $\Delta T$  is the global mean temperature bias at a given atmospheric level), the remaining regional bias patterns are reduced in the corrected simulations except very close to the surface, as can be seen in Figure 6 that displays the RMSE of this centered temperature  $\tilde{T}$ . In this case the iterative run-time bias correction procedure leads to further improvement in most parts of atmosphere above about 900 hPa (with the exception of a small degradation of the biases at about 850 hPa, which are already  
165 not well corrected in  $C_0$ , and an already-mentioned degradation at about 150 hPa). This means that, while the global mean temperature biases – predominantly cold below about 150 hPa and very likely caused by deficiencies in the model physics – are not corrected, regional-scale temperature bias patterns are smoothed because of the corrected model dynamics.

Sea-level pressure biases are only weakly reduced in our simulations that only bias-correct wind patterns. In  $C_0$ , the global RMSE of the annual mean sea-level pressure (with respect to ERA5) is reduced by 10% compared to the uncorrected control  
170 simulation M, and iterations of the bias correction method only lead to insignificant overall improvements (the reduction compared to M is 13% for simulation  $C_3$ ). The weak correction of sea-level pressure errors is in contrast to earlier results for the Southern Hemisphere obtained using run-time temperature corrections (Krinner et al., 2019).

### 3.3 Monthly to interannual circulation variability

As stated, building on cyclostationary correction terms, the run-time bias correction procedure used here is, by construction,  
175 designed to better represent climatological mean values of the corrected variables. However, it is certainly of equal importance to assess whether these run-time bias corrections also improve the way the model represents circulation variability on different timescales.

The dominant patterns of interannual variability of monthly circulation structures are indeed more realistically depicted in the corrected simulations  $C_0$  than in the uncorrected control simulations M, and even more so in simulations with iterated run-time  
180 bias corrections ( $C_{1-3}$ ). This can be seen in Table 2 that displays the seasonal squared spatial Pearson correlation coefficient

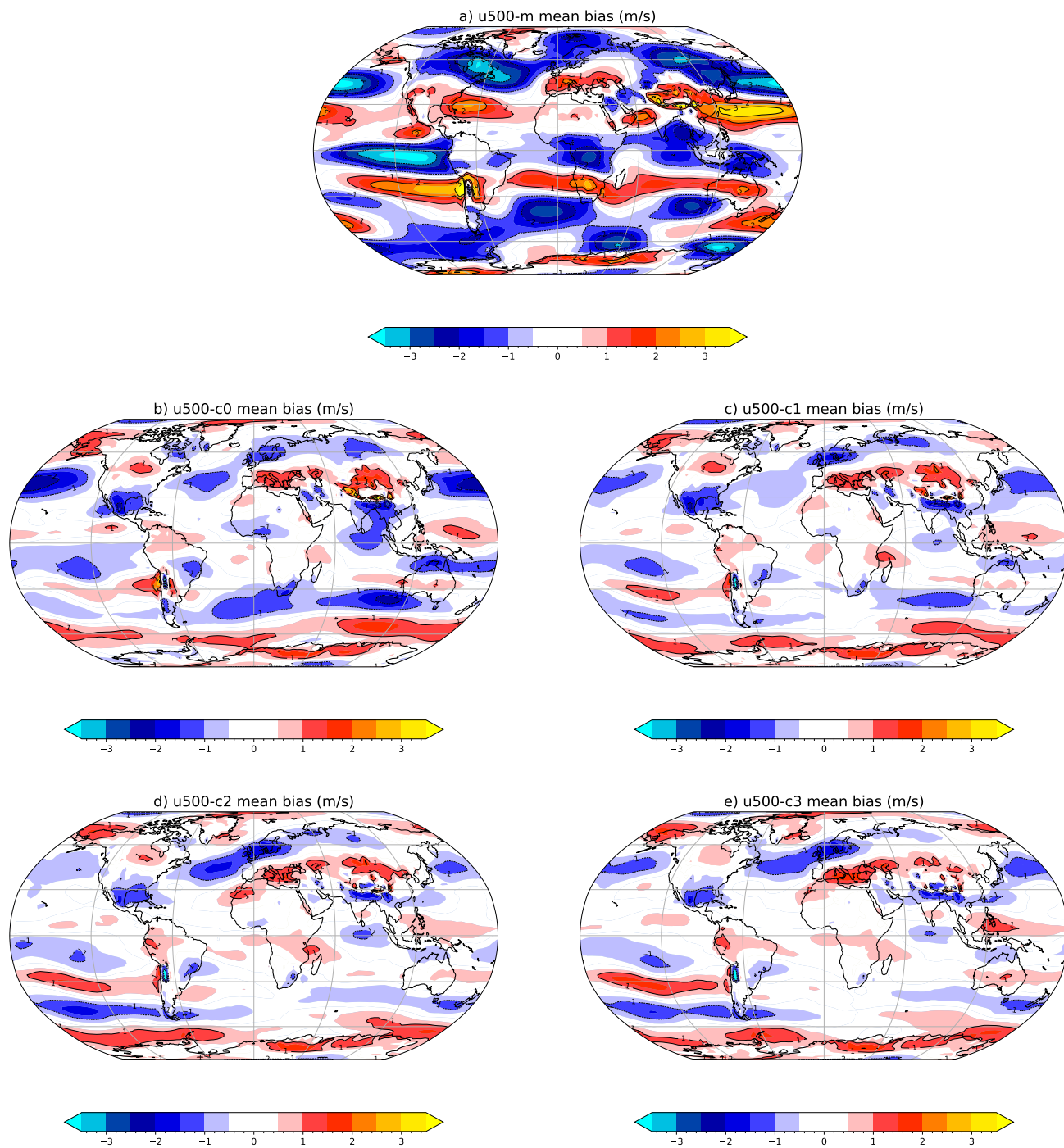


**Figure 3.** Annual mean 500 hPa zonal wind mean bias with respect to ERA5 (in  $\text{ms}^{-1}$ ), for different simulations. a) uncorrected control simulation M; b) corrected simulation  $C_0$ ; c) first iterated corrected simulation  $C_1$ ; d) second iterated corrected simulation  $C_2$ ; e) third iterated corrected simulation  $C_3$ .

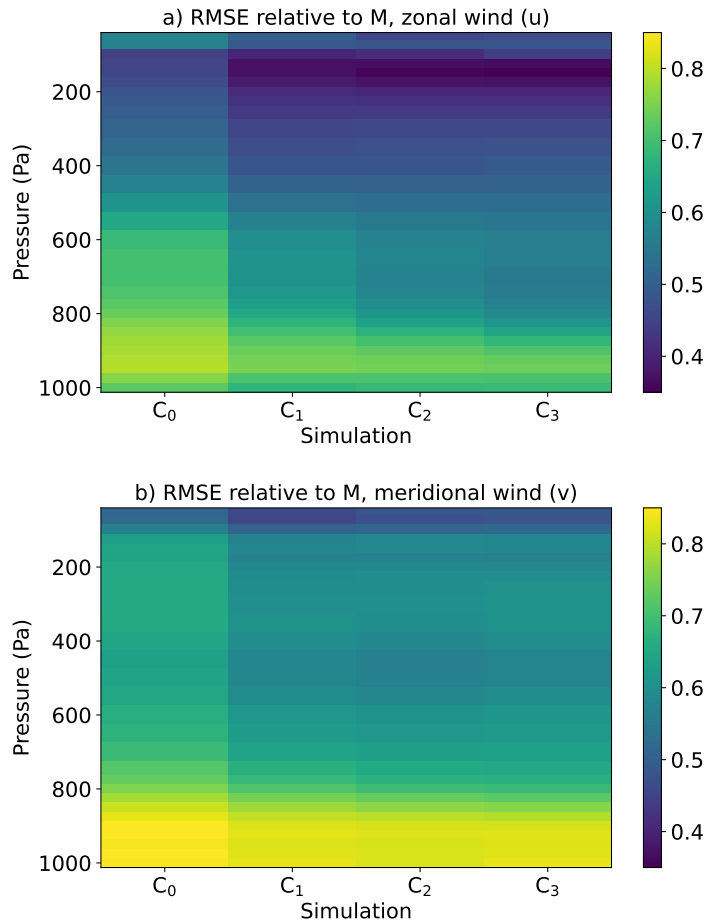


**Figure 4.** Annual mean of monthly mean RMSE (with respect to ERA5) for zonal (a) and meridional (b) wind, for the corrected simulations C<sub>0</sub>–C<sub>3</sub>, relative to the same quantity for the uncorrected control simulation M. Values below 1 indicate that the RMSE in the corrected simulations C<sub>i</sub> is smaller than the RMSE of the uncorrected control simulation M.

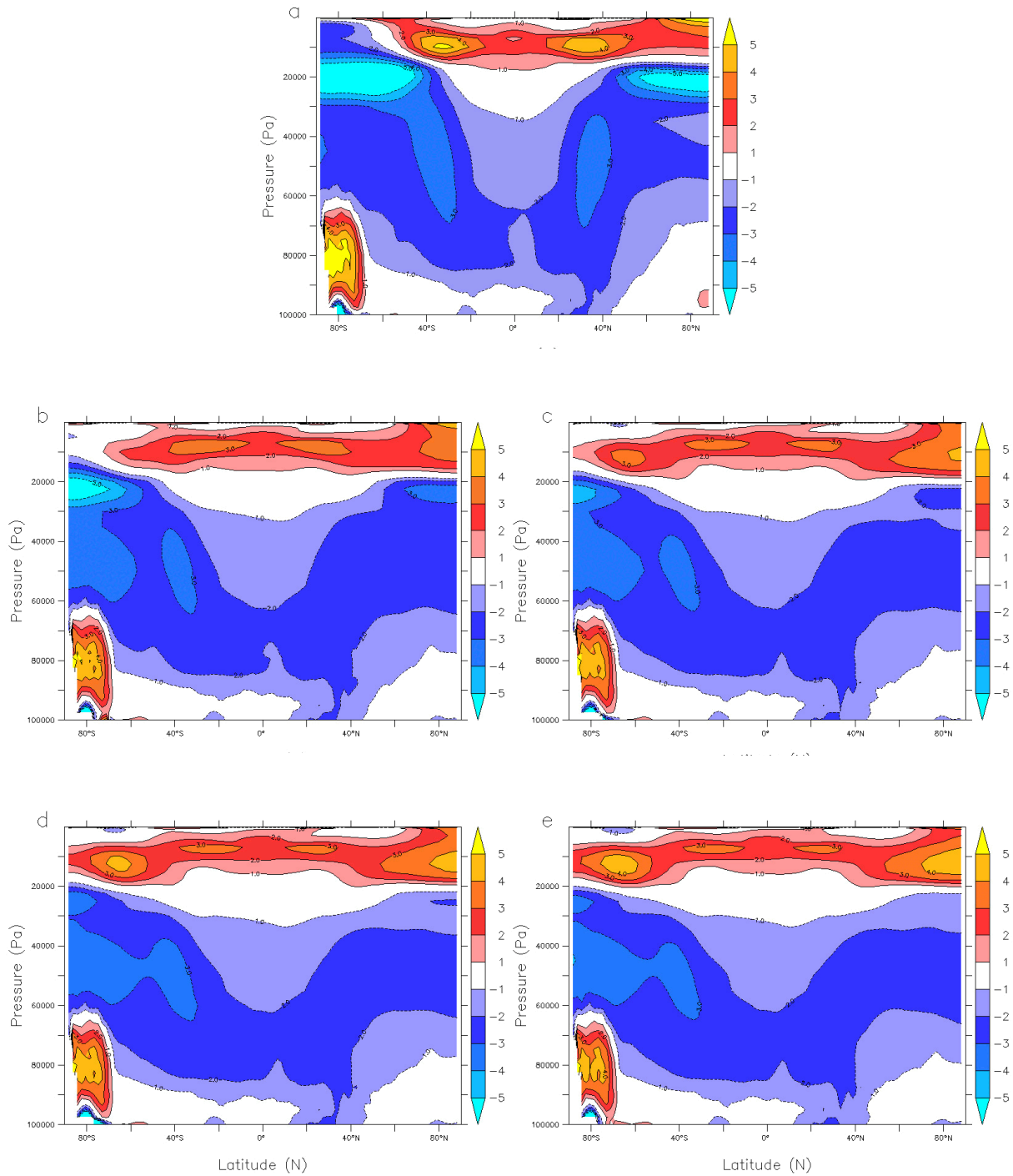


**Figure 5.** Zonal and annual mean temperature biases of the control simulations M (a) and the corrected simulations C<sub>0</sub>-C<sub>3</sub> (b,c,d,e) against ERA5 (°C).

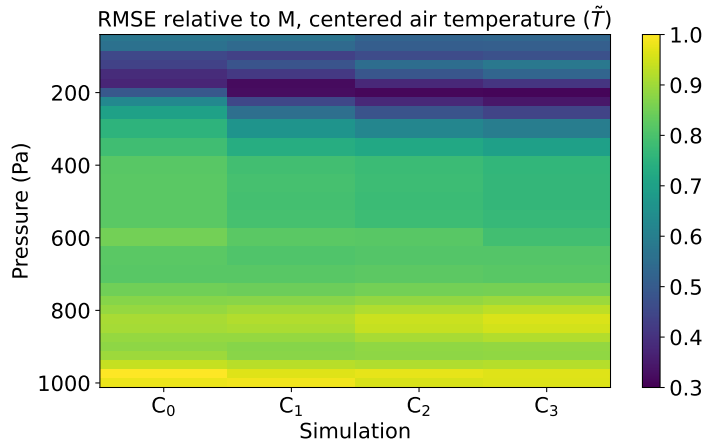


**Figure 6.** Annual mean of monthly mean RMSE (with respect to ERA5) of the centered air temperature  $\tilde{T}$  (see text), for the corrected simulations  $C_{0..3}$ , relative to the same quantity for the uncorrected control simulation M, with global mean bias for the respective level subtracted. Values below 1 indicate that the RMSE in the corrected simulations is smaller than the RMSE of the uncorrected control simulation.

$r^2$  between simulated (LMDZ) and “observed” (ERA5) dominant modes of monthly 500 hPa geopotential anomalies, as identified by principal component analysis for the different corrected model runs  $C_i$ , relative to the corresponding squared spatial correlation coefficient for the uncorrected control simulations M:  $R = r_{C_i}^2 / r_M^2$ .

185 Only seasons for which the first principal component explains more than 40% of the variance in the ERA5 dataset are retained here in order to restrict the analysis to the most stable and physically meaningful patterns. Although the 20-year observational period might be a bit short and could be the reason for some remaining noise in the results reported in Table 2 – the tendencies for a given season and hemisphere from  $C_0$  to  $C_3$  are not always steady –, it seems that an iteration of the run-time bias correction leads in most cases to a better representation of the interannual circulation variability patterns. The results reported here are obtained for the total 40 years of the two 20-year runs of each experiment  $C_i$ , but the results for individual  
190 20-year runs of these experiments are very similar, increasing the confidence in the robustness of the results. Furthermore, the squared correlation coefficients overall increase between  $C_1$  and  $C_2$ .

### 3.4 Short-term circulation variability

195 Diagnostics of short-term atmospheric circulation variability indicate an overall positive impact of the wind-based bias corrections for spatial means of bandpass-filtered extratropical winter sea-level pressure variability and average blocking frequencies (Table 3), but there is no clear improvement over multiple iterations of the correction procedure.

The winter short-term (2.5–8 day) mid-latitude (40–60°N and 40–60°S) sea-level pressure variability, diagnosed from the temporal standard deviation of sea-level pressure from its seasonal mean ( $\sigma_{2.5-8d}$ , using a bandpass filtering in the frequency domain, and limited to grid points with surface height below 1000 m) shows no consistent improvement, and even slight

Hemisphere and season	$R = r^2/r_M^2$				$r_M^2$
	$C_0$	$C_1$	$C_2$	$C_3$	
30-90°N, MAM	1.19	<b>1.19</b>	1.12	1.14	0.56
30-90°N, SON	1.06	1.15	1.21	<b>1.24</b>	0.47
30-90°S, DJF	1.03	0.96	<b>1.03</b>	1.01	0.76
30-90°S, JJA	1.13	1.24	1.24	<b>1.25</b>	0.54
30-90°S, SON	1.12	1.23	<b>1.24</b>	1.18	0.49

**Table 2.** Squared spatial correlation coefficient  $r^2$  between the corrected LMDZ runs  $C_i$  ( $i=0, \dots, 3$ ) and ERA5, for the first EOF of monthly extratropical (30-90° latitude) variability of the 500 hPa geopotential height ( $\phi_{500\text{hPa}}$ ) for selected seasons and hemispheres, 2001-2020, relative to the corresponding squared correlation coefficient  $r_M^2$  of the uncorrected control simulation M:  $R = r_{C_i}^2/r_M^2$ . Only cases for which the variance explained in the ERA5 reanalysis exceeds 40% are shown. The squared spatial correlation coefficient for the uncorrected control simulation M,  $r_M^2$ , is given in the last column for reference. The corrected simulation with the highest relative  $r^2$  is bolded (although differences between simulations are not necessarily significant).

degradation, for the iterated corrections  $C_{1\dots3}$  compared to the simple non-iterated bias correction applied in  $C_0$ . However, the short-term pressure variability is overall better depicted in the corrected than in the uncorrected control simulations.

Blocking anticyclones are a significant atmospheric phenomenon, although there is not one standard accepted definition (Lupo, 2021). Here we follow the widely used definition by Davini et al. (2012): Blocking events are diagnosed at a given point in time and space based on the reversal of the meridional gradient of geopotential height measured at 500 hPa, extending over at least 15° of continuous longitude, and persisting within a 5° latitude  $\times$  10° longitude box centered on a given grid point for at least 5 days. We then calculate the annual mean frequency of these events for each grid point, and calculate the spatial RMSE  $E$  of these frequencies compared to ERA5. For each corrected simulation, the ratio between  $E_{C_i}$  for that simulation and  $E_M$  of the uncorrected control simulation is then computed, yielding a score  $f_B = E_{C_i}/E_M$ . While the iterated procedure seems to improve the model score for the 30-75°N annual and spatial mean blocking frequency, (i.e.,  $f_B$  (30-75°N) < 1), with best results obtained for 2 and 3 iterations, the bias-corrected simulations show degraded performance compared to the uncorrected control simulations (i.e.,  $f_B$  (30-75°S) > 1) in the Southern Hemisphere (30-75°S). However, in the Southern Hemisphere, the iterated bias correction procedure leads to less degraded performance compared to a single bias correction in  $C_0$ .

In the Southern Hemisphere, the mean RMSE of the frequencies of typical hemispheric-scale daily circulation patterns, as identified using 20 (5x4) self-organizing maps for each season (DJF and JJA) and denoted as  $f_S$  in Table 3, is slightly degraded in the corrected simulations compared to the uncorrected control simulation (see  $f_S$  for 40-90°S in the table). Frequency errors are increased by about 15% on average compared to the uncorrected control simulation. Iterations of the bias correction procedure ( $C_{1\dots3}$ ) do not show any consistent change (neither improvement nor degradation) compared to the non-iterated bias correction applied in  $C_0$ , even if  $C_2$  and  $C_3$  show the least degradation in JJA and DJF, respectively, compared to  $C_0$ . In the

Northern Hemisphere, the non-iterated bias correction  $C_0$  procedure produces the best results of all simulations (including the uncorrected control simulation M). In other words, while the bias correction method appears to improve the model performance in this particular respect, iterating the bias correction procedure does not lead to further improvement of the frequency of the simulated main synoptic weather patterns (see  $f_S$  for 40-90°S in the table).

Overall, taking these diagnostics together, the wind bias correction does lead to a modestly improved representation of short-term atmospheric circulation variability, but iterating the bias correction procedure does not necessarily lead to clear further improvement. We note that in the cases where the model performance is degraded by applying the bias correction once (that is,  $C_0$  shows degraded performance relative to M), iterating the bias correction can lead to improved (less degraded) results.

Variable	$C_0$	$C_1$	$C_2$	$C_3$
$\sigma_{2.5-8d}(p_{msl})$ (DJF 40-60°N)	0.94	0.97	1.00	<b>0.94</b>
$\sigma_{2.5-8d}(p_{msl})$ (JJA 40-60°S)	<b>0.96</b>	0.96	1.06	1.03
$f_B$ (30-75°N)	0.83	0.86	<b>0.69</b>	0.75
$f_B$ (30-75°S)	1.18	1.09	<b>1.06</b>	1.08
$f_S$ (DJF 40-90°S)	1.14	1.24	1.09	<b>1.07</b>
$f_S$ (JJA 40-90°S)	1.14	1.14	<b>1.04</b>	1.15
$f_S$ (DJF 40-90°N)	<b>0.76</b>	0.91	0.79	0.86
$f_S$ (JJA 40-90°N)	<b>0.88</b>	1.01	1.03	0.95

**Table 3.** RMSE of selected model results, calculated with respect to ERA5 (2001-2020) and normalized with respect to the uncorrected control simulations M, for high-frequency circulation-related quantities.  $\sigma_{2.5-8d}(p_{msl})$ : bandpass-filtered (between 2.5 and 8 d) sea-level pressure standard deviation between 40 and 60° latitude in both hemispheres, limited to grid points below 1000 m surface height;  $f_B$ : annual mean frequency of blocking situations (based on daily mean 500 hPa geopotential height) between 30 and 75°N and S;  $f_S$ : individual frequencies of the 20 most representative hemispheric extratropical large-scale synoptic situations based on daily 500 hPa geopotential maps. The simulation with the lowest RMSE of the corrected simulations is bolded (note however that values  $> 1$  indicate that the model performance is degraded with respect to the uncorrected control simulations M). Differences between simulations are not necessarily significant.

## 4 Discussion

### 4.1 Limitations linked to the design of the model simulations

#### 4.1.1 Simulation periods: Length of the calibration and evaluation periods

We made the choice in this study to calibrate the bias-correction terms over the 1981–2000 period and to evaluate the effect of the bias correction for the out-of-sample period 2001–2020. This means that both periods only cover 20 years, albeit with two model realizations for the evaluation runs. Although 20 years is today often considered to be a reasonably long evaluation period – see for example the IPCC AR6 WGI model evaluation chapter (Eyring et al., 2021) –, one might wonder whether

a longer calibration period would lead to substantially different results. However, there is a definite risk of over-correction  
235 when too long a calibration period is used, if only because this limits the possibility for out-of-sample testing. Of course this  
does not mean that a longer calibration period of 30 years would not be preferable when applying this method, as long as the  
conclusions for the experiment setup that have been drawn here with clear out-of-sample evaluation are kept in mind.

#### 4.1.2 Model resolution

These simulations have been carried out at a rather low horizontal resolution of  $3.75^\circ$  (longitude)  $\times$   $1.875^\circ$  (latitude), lower  
240 than the standard IPSL-CM6A-LR setup used in CMIP6 (Bonnet et al., 2021) with its  $2.5^\circ \times 1.25^\circ$ . However, the vertical  
resolution, with 79 levels, corresponds to the standard CMIP6 setup for this model in order to reduce the need for re-tuning of  
the physical parametrisations. The reason for this choice is of course computational efficiency. Many model biases have similar  
structures at varying resolution, even if their amplitude can vary. The point here is to evaluate the benefit of iterated run-time  
bias corrections, rather than an optimum model setup with as weak as possible initial model biases. We are therefore fairly  
245 confident that our main results and conclusions remain valid at a higher horizontal resolution.

#### 4.1.3 Choice of bias-corrected variables

Focusing on polar regions (Krinner et al., 2019), previous studies with empirical run-time corrections of wind and temperature  
in the LMDZ AGCM have yielded promising results. However, at least with the most recent version of the LMDZ AGCM, we  
have found strong detrimental effects of temperature corrections in the lower latitudes. As shown in Figure 5, LMDZ has a  
250 wide-spread cold bias of about  $2^\circ\text{C}$  in the mid-troposphere. Empirical run-time corrections of this bias physically correspond to  
an additional radiative heating. As mentioned before (section 2), we suspect that this leads to a weakening of the temperature  
lapse rate and reduced convective activity. As a result, humidity accumulates in the lower troposphere, which reduces the  
upwards surface latent heat flux on large scales, in particular over the oceans, and the (approximate) global surface energy  
balance is strongly perturbed - in an ocean-atmosphere coupled model, this would lead to a very strong oceanic warming  
255 exceeding by far the observed oceanic heat uptake (von Schuckmann et al., 2023).

It is noteworthy that this destructive effect of empirical temperature correction is highly model-dependent. For example, no  
such effect has been noted in various versions of the Canadian atmospheric model CanAM (Krinner et al., 2020; Scinocca and  
Kharin, 2024). It is very likely that the package of physical parameterizations in LMDZ causes this cold bias, and at the same  
time counteracts temperature ERBC because it was consistently developed and tuned to comply with a certain set of observed  
260 metrics, on particular TOA radiative fluxes (Hourdin et al., 2021). In this model, complying with these radiative metrics appears  
to be in contradiction with an absence of a pervasive cold bias in the mid-troposphere, as tests of tuning strategies to eliminate  
the cold bias did not yield satisfying results in terms of TOA radiative metrics. We have to leave this problem unsolved for  
future work.

This motivated the choice to only bias-correct the wind in this study. As a consequence, as shown above, the widespread  
265 cold bias in the mid-troposphere is not corrected. Of course this raises questions about the usefulness of such bias-corrected  
simulations for driving limited-area models for simulations of the present climate and projections. The uncorrected large-scale

cold bias of LMDZ would certainly also lead to a cold bias in the nested limited-area model which would, in most cases, not be able to correct for the bias through its own, possibly less biased, radiative-convective process representations, given the time scales of atmospheric circulation involved (see Labonté et al., 2025; Scinocca et al., 2025). If the aim of the bias-corrected simulations is to serve as boundary conditions for a regional climate model, then the relevant criterion will be the quality of the lateral boundary conditions ( $u$ ,  $v$ ,  $T$ ,  $q$ ) provided to the regional model rather than the internal physical behaviour of the global model, justifying temperature ERBC in LMDZ in spite of perturbed physics. But the aim of the present paper is to present the iterative ERBC method as such. Therefore, we limited the ERBC here to the zonal and meridional wind components.

The choice to only correct the horizontal wind components, and not other variables such as temperature or atmospheric humidity, can make sense if one thinks of the partly conceptual separation between model dynamics and physics. The horizontal wind components, in particular above the atmospheric boundary layer, are quite directly determined by the model dynamics. Atmospheric temperature and humidity, in contrast, and in particular on large spatial scales, can be seen as primarily determined by the model physics. One can argue that the pervasive cold bias throughout the almost entire mid-troposphere, partly “hidden” by stronger local temperature biases caused e.g. by the latitudinal misplacement of jet streams, should be preferably corrected by improved model physics or specific tuning. In contrast, localized biases caused by the misplacement of circulation features are often resolution-dependent and as such more obvious aims for empirical run-time bias corrections limited to the horizontal wind components. It can therefore make sense to separate atmospheric circulation structures from other variables such as temperature and humidity in bias-correction approaches. The effect of misplaced circulation features (for example, a misplaced storm track) often cannot be corrected a posteriori (see an example by Maraun et al. (2017)), while a posteriori bias corrections of “physical” variables related to surface climate, such as temperature and precipitation, are quite usual.

## 4.2 Effect of the nudging time constant $\tau$

In studies using the nudging technique, the optimal choice of the nudging time constant  $\tau$ , and more generally of technical choices in the implementation of the nudging procedure, has repeatedly been the object of attention (e.g., Kruse et al., 2022; Zhang et al., 2022; Scinocca and Kharin, 2024). Tests of a range of different nudging time constants  $\tau$  within the rather usual range between 1 and 3 days, both for the non-iterated and the iterated bias correction procedure, have shown that  $\tau = 1$  d overall yields the best results in our modeling framework consisting of nudging wind in the LMDZ AGCM (Champouillon et al., 2026), at least for the range of time constants tested here. Scinocca and Kharin (2024) show that under certain conditions small nudging time constants (below  $\tau = 1$  d) can lead to strongly degraded ERBC results. However, in a study of the effect of “classical” ERBCs on the simulation of the Antarctic climate (Krinner et al., 2019), a nudging timescale of  $\tau = 6h$  was used, substantially less than that used here ( $\tau = 1$  d), and that in that study, improvements of the simulated climate were shown across all timescales, including high-frequency variability. We note in this respect that the iterative procedure used here can be seen as a method that leads to a stronger effective nudging, as shown by the fact that the amplitude of the combined correction terms  $G_{0+\dots+i}$  for higher numbers  $i$  of iterations increases (see Figure 2). Additional systematic tests of the effects of smaller time constants  $\tau < 1$  d in LMDZ are planned for future studies.

300 Related to this question, it is interesting to ask whether an iterated bias correction with a larger time constant  $\tau$  could actually be a simple equivalent of a “classical” non-iterated bias-correction with a correspondingly smaller time constant. Figure 7 shows that this is not the case: it displays the ratio between the bias correction increments in a “classical” non-iterated simulation with  $\tau = 1$  d (as in the rest of the simulations discussed in detail in this paper), relative to the increments used in a supplementary, twice iterated bias-corrected simulation with  $\tau = 3$  d (which uses three nudging simulations instead of  
 305 only one). This clearly shows that the iteration procedure is not equivalent to a non-iterated bias correction procedure with a correspondingly smaller nudging time constant. A more detailed comparison of these simulations with different nudging time constants and numbers of iterations is provided in Champouillon et al. (2026).

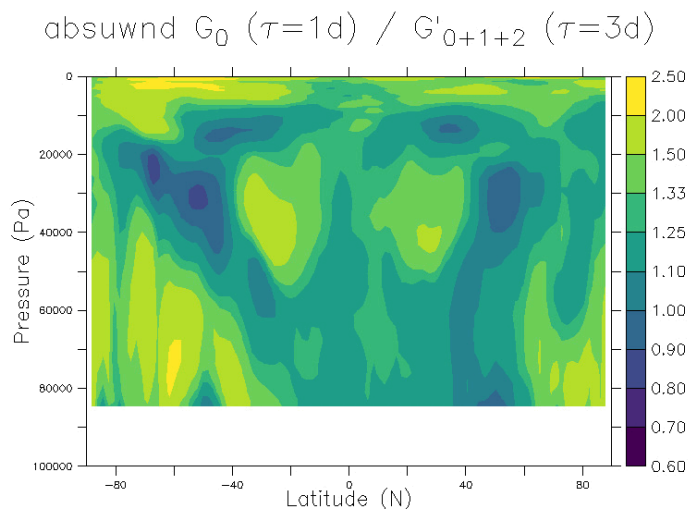


**Figure 7.** Ratio of the zonal mean absolute zonal wind bias correction increments  $G$  (annual mean for 1981 to 2000) between those used for  $C_0$  (noted  $G_0$ , with  $\tau = 1$  d, as in the rest of this paper) and those used in a supplementary test simulation with twice iterated bias corrections and  $\tau = 3$  d (noted  $G'_{0+1+2}$ ). Values between 100000 and 85000 Pa are not shown in the lower part of the figure. They are not relevant as, by construction, the absolute values of the increments vanish at these altitudes (see Figure 1).

### 4.3 Over-correction: Out-of-sample vs. in-sample evaluation

An obvious risk of iterative bias correction procedures is over-correction of model biases, leading to degraded or physically  
 310 less meaningful results when the model is applied outside of the calibration period. To detect possible signs of over-correction, the difference of the global mean RMSE reduction in corrected simulations between the calibration period (1981–2000, “in-sample”) and the normal evaluation period (2001–2020, “out of sample”) is displayed in Figure 8 for mean annual zonal and meridional wind speed at different levels in the atmosphere. The idea is that if, as the number of iterations increases, the

performance during the out-of-sample period (2001-2020) is systematically degrading compared to the performance during  
315 the in-sample period (1981-2000), then this means that the real added value of additional iterations is decreasing. As Figure  
8 suggests, this seems to be the case at least after three iterations. In that case, while for several variables the in-sample score  
still continues to increase, the out-of-sample score starts to decrease. This is particularly the case for variables which have low  
overall bias reduction scores, for example the 700 hPa meridional wind. The difference between the evolution of the in-sample  
and the out-of-sample scores is weaker for variables which have strong bias correction scores, such as the 200 hPa zonal wind.

320 It therefore seems that after about three iterations of the bias-correction method, the performance during the out-of-sample  
period is degrading compared to the performance during the in-sample period, in particular for variables for which still some  
potential for correction is left. As a precaution, we interpret this as a sign of over-correction, suggesting that two iterations of  
the bias correction method should be the maximum number in practical applications.

It is possible, however, that there is some interference between possible over-correction and the fact that the study period,  
325 1981–2020, is a period of strong climatic change. Although it has been shown before that nudging-based ERBC remains valid  
under strong climate change (Krinner et al., 2020), part of the performance over the 2001–2020 period might therefore be  
influenced by the climate change signal. One could, as an additional test, use 2001–2020 as the ERBC calibration period and  
1981-2000 for validation, or use pair years between 1981 and 2020 for the ERBC calibration and odd years of the same period  
for out-of-sample testing. However, the main motivation for our use of various ERBC approaches is to eventually use it in  
330 climate change simulations. In that sense, evaluating the effect of the bias corrections in a climate that is warmer than the  
calibration period, but still known, is a relevant test for the intended use of the ERBC approach.

#### 4.4 Persistence and attenuation of bias patterns

We have shown that globally the mean biases are progressively reduced during the iteration of the bias correction, at least until  
the point when over-correction starts to occur. However, it is clear that the overall structure of the bias patterns is robust, as  
335 can be seen very clearly for example in Figure 3. This is not surprising, as climate model bias patterns are quite persistent even  
under strong climate change (Krinner and Flanner, 2018; Krinner et al., 2020).

What is noteworthy nevertheless is that the strength of attenuation of mean biases is to some degree spatially variable. For  
example, while Figure 3 shows a steady decrease of the annual mean 500 hPa zonal wind mean bias in the Southern Indian  
Ocean with increasing number of iterations of the bias correction, the corresponding bias pattern over Western Europe (positive  
340 over the Mediterranean and negative over North-western Europe) quickly stabilises, and is even amplified in simulations  $C_2$  and  
 $C_3$  relative to  $C_0$  and  $C_1$ . Similarly, while biases continue to decrease over the North Pacific, they already start to re-increase  
in simulation  $C_2$  over the South Pacific. The reasons for regional persistence of biases are not clear, and they probably are  
region-specific. It is for example possible that these regionally varying behaviours are linked to region-specific factors such as  
topography, or that they are caused by teleconnection patterns in interaction with error compensation (in the sense that in two  
345 regions linked by teleconnection mechanisms, well correcting an error in one region might unmask errors in the other region).

As a consequence, iterating the bias correction method might allow regional climate modelers to dispose of much improved  
atmospheric boundary conditions for the RCM in one specific region, but not in another. A detailed analysis for the reasons of

bias persistence in specific regions is beyond the scope of this paper, and these reasons can depend on various factors, possibly including resolution, and are probably model-dependent. Regional bias persistence in different variations of ERBC is analysed in more detail in Champouillon et al. (2026).

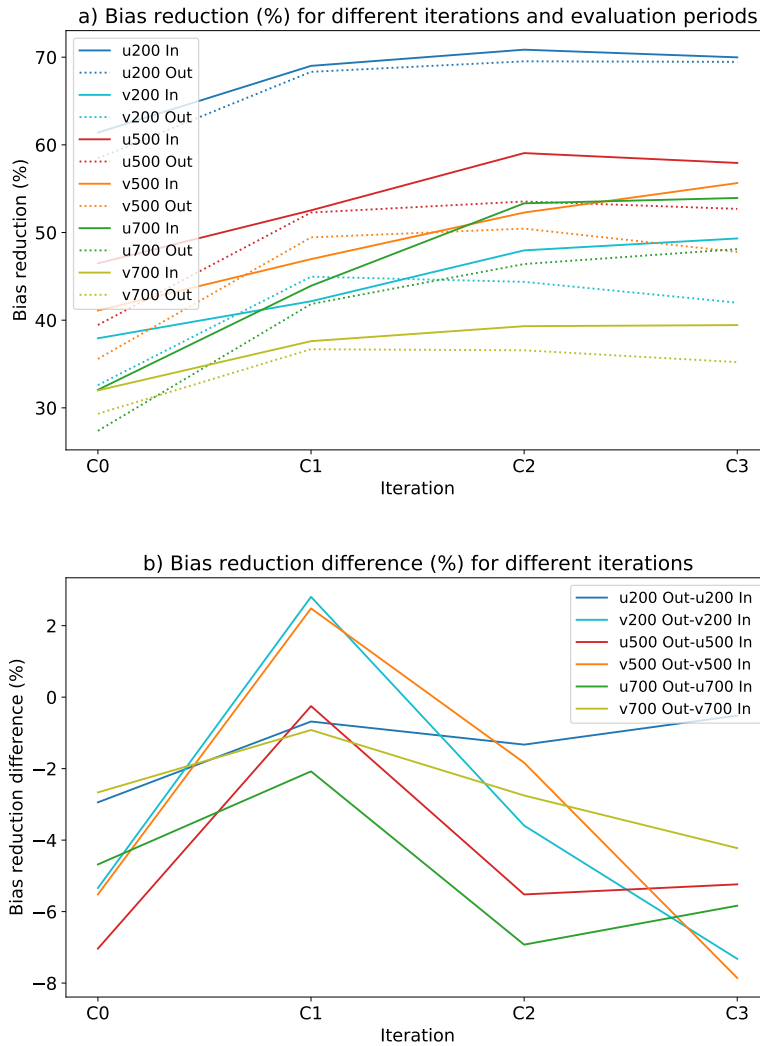


**Figure 8.** Comparison of bias reduction compared to the uncorrected control simulation M (in %) between different evaluation periods. a) Bias reduction for in-sample and out-of-sample periods, for each variable; b) Difference between in-sample and out-of-sample periods, for a given variable. As the model is nudged during the years 1981–2000, the period 1981–2020 corresponds to in-sample evaluation (noted “In”), while 2001–2020 corresponds to out-of-sample evaluation (noted “Out”).

## 4.5 Simple multiplication of correction increments

As we have shown here (see for example Figure 3), the geographical patterns of the mean model biases are somewhat independent of the number of iterations, and the mean absolute bias correction increments increase with the number of iterations (see Figure 2). This might suggest that as a first simple approach one could try to use a multiple of the bias correction terms obtained during the first nudging (that is, those applied in  $C_0$ ) as a surrogate for the more costly iteration procedure. We have carried out a simple test in which the correction terms of  $C_0$  are amplified by 50%; otherwise this simulation (referred to as  $C_{0,\times 1.5}$  in the following) is identical to  $C_0$ . The analysis of  $C_{0,\times 1.5}$  shows that the bias correction is less efficient than in  $C_0$ . For example, with respect to ERA5, the annual mean global RMSE of the 500 hPa zonal and meridional wind components is 7.5% ( $u_{500}$ ) and 15.6% ( $v_{500}$ ) higher in  $C_{0,\times 1.5}$  than in  $C_0$ . However we note that  $C_{0,\times 1.5}$  still shows a substantial improvement compared to the uncorrected model run M.

It is fairly easy to understand why the model performance degrades between  $C_0$  and  $C_{0,\times 1.5}$ . As one can see in Figure 2, although the amplitude of the correction terms does increase essentially everywhere for higher iterations of the correction procedure, the ratio of the correction terms between different phases of the iteration procedure is not uniform – it clearly has a spatial structure. A simple overall increase of the initial correction terms, although modest in our test, does not reproduce this spatial structure.

## 5 Conclusions

This work has shown that iterating the “classical” empirical run-time bias correction method described by Guldberg et al. (2005) once or twice (as in our simulations  $C_1$  and  $C_2$ , respectively) substantially reduces the mean bias of the bias-corrected variables compared to simulations in which the bias correction procedure is not iterated. However, the representation of atmospheric circulation variability on interannual and shorter timescales is not always improved in simulations with iterated bias corrections. Signs of over-correction appear after about three iterations of the bias correction procedure.

All in all, the method described is easy to implement, adds substantial value and does not represent a very high additional cost compared to the non-iterated procedure.

Several other variants or further developments of run-time bias corrections have been proposed, such as a method based on direct compensation of diagnosed model biases (“CABCOR”: Scinocca and Kharin, 2024) or inference of bias-correction terms using machine learning (Watt-Meyer et al., 2021). We have implemented the CABCOR method in LMDZ and found it to yield very good results, in many respects equivalent to the iterative method presented here. We have also developed a method of state-dependent bias corrections based on the simulated instantaneous synoptic situation (as expressed in the regional 500 hPa geopotential field) as a variant of the “classical” nudging-based ERBC. These approaches are evaluated in the context of LMDZ and without temperature correction by Champouillon et al. (2026). In addition, we are currently implementing machine-learning-based inference of state-dependent ERBC in LMDZ, following Watt-Meyer et al. (2021).

More generally, because ERBC implementation choices and thus the corresponding results are at least partly model-dependent, it would be interesting to see the effect of iterative ERBC in other models, possibly in the framework of a coordinated multi-model intercomparison of various ERBC methods.

385 *Code and data availability.* Configuration files and model code changes, scripts and model output data used to plot the graphics are available on Zenodo under doi:10.5281/zenodo.16363995 (Krunner, 2025a). The modipsl code infrastructure required to compile the codes, including the full model code (in particular LMDZ v6.3 but also ORCHIDEE and XIOS), is available on Zenodo under doi:10.5281/zenodo.17381280 (Krunner, 2025b).

390 *Author contributions.* GK designed the study, carried out the simulations, contributed to the analysis, and wrote the first draft of this article. AC contributed to the analysis and writing. JB and FC contributed to writing and overall discussions about the method.

*Competing interests.* The authors declare no competing interests.

*Acknowledgements.* This study has received funding from Agence Nationale de la Recherche – France 2030 as part of the PEPR TRACCS programme under the grants ANR-22-EXTR-0005, ANR-22-EXTR-0008, ANR-22-EXTR-0010, and ANR-22-EXTR-0011. It was provided  
395 with HPC computing and storage resources by GENCI at TGCC under the grants 2024-A0180116219 and 2024-AD010101523R on the Joliot Curie supercomputer (SKL and ROME partitions).

## References

- Arias, P. A., Bellouin, N., Coppola, E., Jones, R. G., Krinner, G., Marotzke, J., Naik, V., Palmer, M. D., Plattner, G.-K., Rogelj, J., Rojas, M., Sillmann, J., Storelvmo, T., Thorne, P. W., Trewin, B., et al.: Technical Summary, in: *Climate Change 2021: The Physical Science Basis. Contribution of Working Group I to the Sixth Assessment Report of the Intergovernmental Panel on Climate Change*, edited by Masson-Delmotte, V., Zhai, P., Pirani, A., Connors, S. L., et al., pp. 33–144, Cambridge University Press, Cambridge, UK and New York, NY, USA, <https://doi.org/10.1017/9781009157896.002>, 2021.
- 400 Beaumet, J., Déqué, M., Krinner, G., Agosta, C., and Alias, A.: Effect of prescribed sea surface conditions on the modern and future Antarctic surface climate simulated by the ARPEGE atmosphere general circulation model, *The Cryosphere*, 13, 3023–3043, 2019.
- 405 Bloom, S., Takacs, L., Da Silva, A., and Ledvina, D.: Data assimilation using incremental analysis updates, *Monthly Weather Review*, 124, 1256–1271, 1996.
- Bonnet, R., Boucher, O., Deshayes, J., Gastineau, G., Hourdin, F., Mignot, J., Servonnat, J., and Swingedouw, D.: Presentation and evaluation of the IPSL-CM6A-LR ensemble of extended historical simulations, *Journal of Advances in Modeling Earth Systems*, 13, e2021MS002565, 2021.
- 410 Champouillon, A., Krinner, G., and Blanchet, J.: Intercomparison of run-time bias correction methods in LMDZ\_v6.3, *Geoscientific Model Development*, submitted, 2026.
- Chang, E. K.: Are band-pass variance statistics useful measures of storm track activity? Re-examining storm track variability associated with the NAO using multiple storm track measures, *Climate dynamics*, 33, 277–296, 2009.
- Chang, Y., Schubert, S., Koster, R., Molod, A., and Wang, H.: Tendency bias correction in coupled and uncoupled global climate models with a focus on impacts over North America, *Journal of Climate*, 32, 639–661, 2019.
- 415 D’Andrea, F. and Vautard, R.: Reducing systematic errors by empirically correcting model errors, *Tellus A*, 52, 21–41, 2000.
- Davini, P., Cagnazzo, C., Gualdi, S., and Navarra, A.: Bidimensional diagnostics, variability, and trends of Northern Hemisphere blocking, *Journal of Climate*, 25, 6496–6509, 2012.
- Doblas-Reyes, F., Sörensson, A., Almazroui, M., Dosio, A., Gutowski, W., Haarsma, R., Hamdi, R., Hewitson, B., Kwon, W.-T., Lamptey, B., Maraun, D., Stephenson, T., Takayabu, I., Terray, L., Turner, A., and Zuo, Z.: Linking Global to Regional Climate Change, in: *Climate Change 2021: The Physical Science Basis. Contribution of Working Group I to the Sixth Assessment Report of the Intergovernmental Panel on Climate Change*, edited by Masson-Delmotte, V., Zhai, P., Pirani, A., Connors, S. L., et al., book section 10, pp. 1363–1512, Cambridge University Press, Cambridge, UK and New York, NY, USA, <https://doi.org/10.1017/9781009157896.012>, 2021.
- 420 Eyring, V., Gillett, N., Achuta Rao, K., Barimalala, R., Barreiro Parrillo, M., Bellouin, N., Cassou, C., Durack, P., Kosaka, Y., McGregor, S., Min, S., Morgenstern, O., and Sun, Y.: Human Influence on the Climate System, in: *Climate Change 2021: The Physical Science Basis. Contribution of Working Group I to the Sixth Assessment Report of the Intergovernmental Panel on Climate Change*, edited by Masson-Delmotte, V., Zhai, P., Pirani, A., Connors, S. L., et al., book section 3, pp. 423–551, Cambridge University Press, Cambridge, UK and New York, NY, USA, <https://doi.org/10.1017/9781009157896.005>, 2021.
- 425 Eyring, V., Gillett, N., Achuta Rao, K., Barimalala, R., Barreiro Parrillo, M., Bellouin, N., Cassou, C., Durack, P., Kosaka, Y., McGregor, S., Min, S., Morgenstern, O., and Sun, Y.: Human Influence on the Climate System, in: *Climate Change 2021: The Physical Science Basis. Contribution of Working Group I to the Sixth Assessment Report of the Intergovernmental Panel on Climate Change*, edited by Masson-Delmotte, V., Zhai, P., Pirani, A., Connors, S. L., et al., book section 3, pp. 423–551, Cambridge University Press, Cambridge, UK and New York, NY, USA, <https://doi.org/10.1017/9781009157896.005>, 2021.
- Guldberg, A., Kaas, E., Déqué, M., Yang, S., and Thorsen, S. V.: Reduction of systematic errors by empirical model correction: impact on seasonal prediction skill, *Tellus A*, 57, 575–588, <https://doi.org/10.1111/j.1600-0870.2005.00120.x>, 2005.
- 430 Hall, A.: Projecting regional change, *Science*, 346, 1461–1462, 2014.
- Hersbach, H., Bell, B., Berrisford, P., Hirahara, S., Horányi, A., Muñoz-Sabater, J., Nicolas, J., Peubey, C., Radu, R., Schepers, D., et al.: The ERA5 global reanalysis, *Quarterly Journal of the Royal Meteorological Society*, 146, 1999–2049, 2020.

- Hourdin, F., Rio, C., Jam, A., Traore, A.-K., and Musat, I.: Convective boundary layer control of the sea surface temperature in the tropics, *Journal of Advances in Modeling Earth Systems*, 12, e2019MS001 988, 2020.
- Hourdin, F., Williamson, D., Rio, C., Couvreur, F., Roehrig, R., Villefranque, N., Musat, I., Fairhead, L., Diallo, F. B., and Volodina, V.: Process-based climate model development harnessing machine learning: II. Model calibration from single column to global, *Journal of Advances in Modeling Earth Systems*, 13, e2020MS002 225, 2021.
- Jeuken, A., Siegmund, P., Heijboer, L., Feichter, J., and Bengtsson, L.: On the potential of assimilating meteorological analyses in a global climate model for the purpose of model validation, *Journal of Geophysical Research: Atmospheres*, 101, 16 939–16 950, 1996.
- Kharin, V. and Scinocca, J.: The impact of model fidelity on seasonal predictive skill, *Geophysical research letters*, 39, 2012.
- Kohonen, T.: Self-organized formation of topologically correct feature maps, *Biol. Cybern.*, 43, 59–69, 1982.
- Krinner, G.: Krinner et al., Iterative run-time bias corrections in an atmospheric GCM (LMDZ v6.3) - LMDZ configuration files, output data and analysis scripts, Zenodo Dataset, doi=10.5281/zenodo.16363996, 2025a.
- Krinner, G.: Krinner et al., Iterative run-time bias corrections in an atmospheric GCM (LMDZ v6.3) - model infrastructure and code, Zenodo Dataset, doi=10.5281/zenodo.17381281, 2025b.
- Krinner, G. and Flanner, M. G.: Striking stationarity of large-scale climate model bias patterns under strong climate change, *Proceedings of the National Academy of Sciences*, 115, 9462–9466, 2018.
- Krinner, G., Viovy, N., de Noblet-Ducoudré, N., Ogée, J., Polcher, J., Friedlingstein, P., Ciais, P., Sitch, S., and Prentice, I. C.: A dynamic global vegetation model for studies of the coupled atmosphere-biosphere system, *Global biogeochemical cycles*, 19, 2005.
- Krinner, G., Beaumet, J., Favier, V., Deque, M., and Brutel-Vuilmet, C.: Empirical run-time bias correction for Antarctic regional climate projections with a stretched-grid AGCM, *Journal of Advances in Modeling Earth Systems*, 11, 64–82, 2019.
- Krinner, G., Kharin, V., Roehrig, R., Scinocca, J., and Codron, F.: Historically-based run-time bias corrections substantially improve model projections of 100 years of future climate change, *Communications Earth & Environment*, 1, 29, 2020.
- Kruse, C. G., Bacmeister, J. T., Zarzycki, C. M., Larson, V. E., and Thayer-Calder, K.: Do Nudging Tendencies Depend on the Nudging Timescale Chosen in Atmospheric Models?, *Journal of Advances in Modeling Earth Systems*, 14, e2022MS003 024, <https://doi.org/https://doi.org/10.1029/2022MS003024>, e2022MS003024 2022MS003024, 2022.
- Labonté, M.-P., Matte, D., Paquin, D., Scinocca, J. F., Kharin, V. V., and Jiao, Y.: Runtime bias corrected driving data for regional climate models: regional-scale impacts, *Climate Dynamics*, 63, 1–20, 2025.
- Lee, H., Calvin, K., Dasgupta, D., Krinner, G., Mukherji, A., Thorne, P., Trisos, C., et al.: Climate Change 2023: Synthesis Report. Contribution of Working Groups I, II and III to the Sixth Assessment Report of the Intergovernmental Panel on Climate Change, Intergovernmental Panel on Climate Change (IPCC), Geneva, Switzerland, <https://doi.org/10.59327/IPCC/AR6-9789291691647>, 2023.
- Lupo, A. R.: Atmospheric blocking events: A review, *Annals of the New York Academy of sciences*, 1504, 5–24, 2021.
- Maraun, D., Shepherd, T. G., Widmann, M., Zappa, G., Walton, D., Gutiérrez, J. M., Hagemann, S., Richter, I., Soares, P. M., Hall, A., et al.: Towards process-informed bias correction of climate change simulations, *Nature Climate Change*, 7, 764–773, 2017.
- Palmer, T. E., McSweeney, C. F., Booth, B. B., Priestley, M. D., Davini, P., Brunner, L., Borchert, L., and Menary, M. B.: Performance-based sub-selection of CMIP6 models for impact assessments in Europe, *Earth System Dynamics*, 14, 457–483, 2023.
- Pithan, F., Athanase, M., Dahlke, S., Sánchez-Benítez, A., Shupe, M. D., Sledd, A., Streffing, J., Svensson, G., and Jung, T.: Nudging allows direct evaluation of coupled climate models with in situ observations: a case study from the MOSAiC expedition, *Geoscientific Model Development*, 16, 1857–1873, 2023.

- Ranasinghe, R., Ruane, A., Vautard, R., Arnell, N., Coppola, E., Cruz, F., Dessai, S., Islam, A., Rahimi, M., Ruiz Carrascal, D., Sillmann, J., Sylla, M., Tebaldi, C., Wang, W., and Zaaboul, R.: Climate Change Information for Regional Impact and for Risk Assessment, in: Climate Change 2021: The Physical Science Basis. Contribution of Working Group I to the Sixth Assessment Report of the Intergovernmental Panel on Climate Change, edited by Masson-Delmotte, V., Zhai, P., Pirani, A., Connors, S. L., et al., book section 12, pp. 1767–1925, Cambridge University Press, Cambridge, UK and New York, NY, USA, <https://doi.org/10.1017/9781009157896.014>, 2021.
- 475 Scinocca, J. F. and Kharin, V. V.: Climatological adaptive bias correction of climate models, *Journal of Advances in Modeling Earth Systems*, 16, e2024MS004563, 2024.
- Scinocca, J. F., Kharin, V. V., Matte, D., Jiao, Y., Labonté, M.-P., Qian, M., Paquin, D., Akingunola, A., and Lazare, M.: Runtime bias correction of regional climate model driving data and its continental-scale impacts, *Climate Dynamics*, 63, 462, 2025.
- 480 Sun, J., Zhang, K., Wan, H., Ma, P.-L., Tang, Q., and Zhang, S.: Impact of nudging strategy on the climate representativeness and hindcast skill of constrained EAMv1 simulations, *Journal of Advances in Modeling Earth Systems*, 11, 3911–3933, 2019.
- von Schuckmann, K., Minière, A., Gues, F., Cuesta-Valero, F. J., Kirchengast, G., Adusumilli, S., Straneo, F., Ablain, M., Allan, R. P., Barker, P. M., et al.: Heat stored in the Earth system 1960–2020: where does the energy go?, *Earth System Science Data*, 15, 1675–1709, 2023.
- Watt-Meyer, O., Brenowitz, N. D., Clark, S. K., Henn, B., Kwa, A., McGibbon, J., Perkins, W. A., and Bretherton, C. S.: Correcting  
485 Weather and Climate Models by Machine Learning Nudged Historical Simulations, *Geophysical Research Letters*, 48, e2021GL092555, <https://doi.org/https://doi.org/10.1029/2021GL092555>, e2021GL092555 2021GL092555, 2021.
- Zhang, K., Wan, H., Liu, X., Ghan, S. J., Kooperman, G. J., Ma, P.-L., Rasch, P. J., Neubauer, D., and Lohmann, U.: On the use of nudging for aerosol–climate model intercomparison studies, *Atmospheric Chemistry and Physics*, 14, 8631–8645, 2014.
- Zhang, S., Zhang, K., Wan, H., and Sun, J.: Further improvement and evaluation of nudging in the E3SM Atmosphere Model version 1  
490 (EAMv1): simulations of the mean climate, weather events, and anthropogenic aerosol effects, *Geoscientific Model Development*, 15, 6787–6816, 2022.